

# Effective Optimization of High Voltage Solid-State Lithium Batteries by Using Poly(ethylene oxide)-Based Polymer Electrolyte with Semi-Interpenetrating Network

Gerrit Homann, Lukas Stolz, Kerstin Neuhaus, Martin Winter,\* and Johannes Kasnatscheew\*

Solid polymer electrolytes (SPEs) are promising candidates for the realization of lithium metal batteries. However, the popular SPE based on poly(ethylene oxide) (PEO) reveals a "voltage noise"-failure during charge, for example, with high energy/high voltage electrodes like LiNi<sub>0.6</sub>Mn<sub>0.2</sub>Co<sub>0.2</sub>O<sub>2</sub> (NMC622), which can be attributed to short-circuits via penetrating Li dendrites. This failure disappears when integrating PEO-based SPE in a semi interpenetrating network, which mainly consists of PEO units, as well. In this work, it is shown that this SPE allows performance improvement via elimination of the crystalline domains without significant sacrifice of mechanical integrity. Hence, a highly amorphous SPE can be obtained by a simple increase of plasticizing Li salts, which overall is beneficial, not only for the ionic conductivity, but also the homogeneity, while remaining mechanically stable and solid in its original shape even after storage at 60 °C for 7 days. These aspects are crucial for the performance of the modified SPE as they can suppress the failure-causing Li dendrite penetration while the electrochemical aspects, that is, anodic stability, are rather unaffected by the modification and remain stable (4.6 V vs Li | Li+). Overall, this optimized SPE enables stable cycling performance in NMC622 | SPE | Li cells, even at 40 °C operation temperature.

G. Homann, L. Stolz, Prof. M. Winter, Dr. J. Kasnatscheew Helmholtz-Institute Münster IFK-12 Forschungszentrum Jülich GmbH Corrensstraße 46, Münster 48149, Germany E-mail: m.winter@fz-juelich.de; j.kasnatscheew@fz.juelich.de Dr. K. Neuhaus Institute of Inorganic and Analytic Chemistry University of Münster Corrensstraße 28/30, Münster 48149, Germany Prof. M. Winter MEET Battery Research Center Institute of Physical Chemistry University of Münster Corrensstraße 46, Münster 48149, Germany The ORCID identification number(s) for the author(s) of this article can be found under https://doi.org/10.1002/adfm.202006289.

© 2020 The Authors. Published by Wiley-VCH GmbH. This is an open access article under the terms of the Creative Commons Attribution-NonCommercial-NoDerivs License, which permits use and distribution in any medium, provided the original work is properly cited, the use is non-commercial and no modifications or adaptations are made.

DOI: 10.1002/adfm.202006289

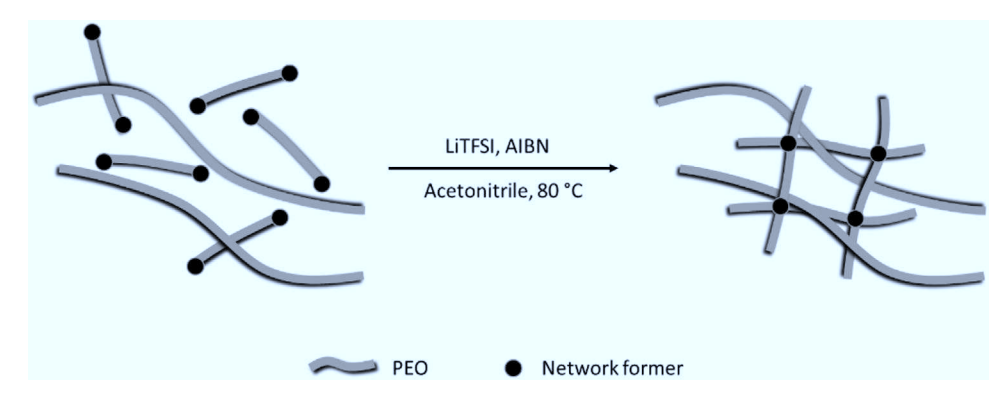
#### 1. Introduction

The substitution of liquid by solid electrolytes in lithium metal batteries (LMB) promises an increase in safety and specific energy (i.e.,in bipolar stacked battery packs).<sup>[1–4]</sup> Identification of a suitable solid electrolyte will be the key for realizing application of Li metal batteries (LMBs).<sup>[5–7]</sup>

Current solid electrolytes can be divided into inorganic (e.g., ceramics, glasses) and organic (e.g., polymers) materials.<sup>[7–9]</sup> Though, some of the inorganic electrolytes can reveal high ionic conductivities, they are typically accompanied with hampered kinetic aspects due to high resistances at particle-particle grain boundaries as well as limited wettability at solid polymer electrolyte (SPE)|electrode interfaces. At contrast, SPEs as representatives of organic solid electrolytes reveal themselves to be particularly advantageous in wettability due to their particle-free and more flexible nature compared to, for example, ceramics. In

addition, feasible processing aspects along with abundant raw materials and rather low required Li concentrations are beneficial in regard to low costs. [10] However, their poor room temperature ionic conductivities (S cm $^{-1}$ ) preferably favor applications using thin electrolyte layers (higher conductance [S]) and/or operation temperatures equal and higher than 60 °C.

Poly(ethylene oxide) (PEO)-based SPE as the popular benchmark system, investigated already since the 1970s, has an application-sufficient interface compatibility with the Li metal electrode<sup>[11]</sup> but is regarded to be unstable with high energy/voltage electrodes, for example, when LiNi<sub>0.6</sub>Mn<sub>0.2</sub>Co<sub>0.2</sub>O<sub>2</sub> (NMC622)<sup>[12–14]</sup> is used as active material.<sup>[15]</sup> Indeed, a thorough investigation in our previous study confirmed a failure in an NMC622|SPE|Li cell, which is visible by an arbitrary appearance of "voltage noise," typically emerging in initial cycles in random manner.[16] Microshorts by Li dendrites, which is a morphology form of high surface area lithium,[17-19] were proven to be the origin of the this voltage noise failure; SPE oxidation as alternative reason for failure could be ruled out.<sup>[16]</sup> This could be evidenced by proper experiments that could eliminate the volta-noise, for example, an exchange of Li with graphite-based negative electrode or by an increase of SPE thickness, both rendering Li dendrites and their



Scheme 1. Synthesis of the s-IPN PEO-based SPE in 2D view. s-IPN can be regarded as trapped PEO chains in a network obtained via polymerization of a network former based on poly(ethylene glycol)dimethacrylate (PEGdMA).<sup>[21]</sup> The formation of the s-IPN is confirmed via the gelation test.

respective penetration difficult.<sup>[16]</sup> In agreement to these findings, the ease of Li denrite penetration through the SPE could be detected and even visualized in proper Li|SPE|Li cells.<sup>[20]</sup>

A solution for overcoming this failure is the integration of the linear, rather soft PEO-based SPE, into a more mechanically robust semi interpenetrating network (s-IPN) (Scheme 1). [21] Still mainly consisting of PEO units, the s-IPN PEO-based SPE can suppress the Li dendrite penetration by improved mechanical rigidness and realize a voltage-noise-free charge/discharge cycling (Figure 1). [21]

The rigid structure of the s-IPN PEO-based SPE restricts the polymer chain mobility, thus decreases the ionic conductivity compared to the linear PEO-based SPE.<sup>[21]</sup> One strategy to increase ionic conductivity is commonly an increased Li salt concentration. However, given the plasticizing effect of the Li salt on the rigid crystalline domains within the polymer matrix, the increase in Li salt concentration is also accompanied with a diminution of mechanical aspects.

In comparison to linear PEO, the mechanical robustness of s-IPN PEO is also given by the network structure, thus is not solely dependent on crystalline domains. This feature reveals a novel opportunity for creating a compromise between ionic conductivity and mechanical properties. Following this proper SPE design and increasing the Li salt concentration we demonstrate excellent cycling stability for high voltage application, that is, in NMC622 SPE Li cells.

#### 2. Experimental Section

#### 2.1. Materials

PEO (MW 300.000 Da), 1-methyl-2-pyrrolidinone (NMP, anhydrous, 99.5%), and poly(ethylene glycol)dimethacrylate (PEGdMA,  $M_{\rm w}$  750 Da) were purchased from Sigma-Aldrich, Germany. Poly(ethylene glycol)dimethacrylate (PEGdMA,  $M_{\rm w}$ 

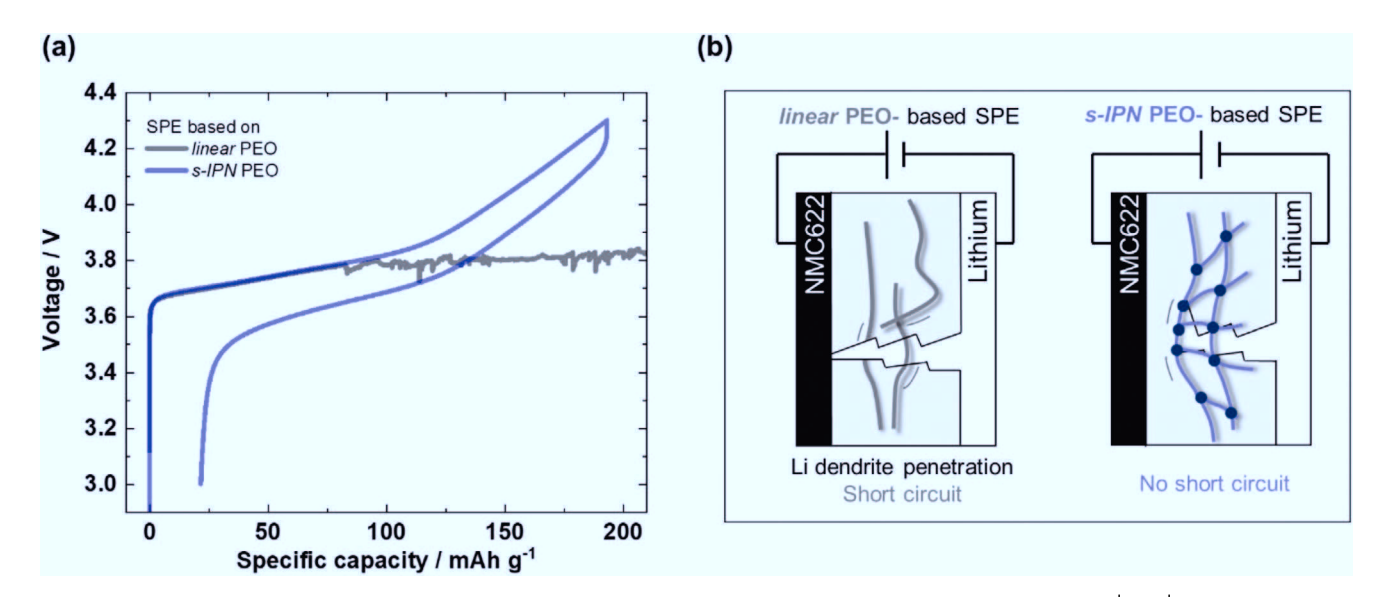


Figure 1. a) Charge/discharge cycle profiles for linear PEO- and s-IPN PEO-based SPEs (4.3–3.0 V; 30 mA  $g^{-1}$ ) in NMC622 | SPE | Li cells at 60 °C. The use of a linear PEO-based SPE results in a failure visible by the random appearance of voltage noise (exemplary profile), [16] while the cell with s-IPN PEO-based SPE operates failure-free. b) As schematically shown, the failure can be attributed to (micro) short circuits originating from Li dendrite penetration through the linear PEO-based SPE, [21] while the SPE based on PEO in an s-IPN network can prevent this penetration and realize charge/discharge cycling without short circuits, thus without voltage noise-failure.

www.afm-journal.de



400 and 1000 Da) were purchased from Polysciences Inc., USA. Lithium bis(trifluoromethanesulfonyl)imide (LiTFSI, 99.9%) and polyvinylidene difluoride (PVdF, Solef 5130) were purchased from Solvay, France. Super C65 carbon black was received from Imerys, France. Mylar foil (100 µm thickness) was purchased from DuPont, USA. Battery grade electrolyte, 1 м LiPF<sub>6</sub> in a mixture of ethylene carbonate and ethyl methyl carbonate (EC/EMC 3:7 by wt.) (LP57 Selectilyte) from BASF, Germany, was used as benchmark liquid electrolyte. The active materials NMC622, LiNi<sub>0.5</sub>Mn<sub>1.5</sub>O<sub>4</sub> (LNMO), LiMn<sub>2</sub>O<sub>4</sub> (LMO), and LiFePO<sub>4</sub> (LFP) were purchased from Targray, Canada. Lithium metal (Albemarle) was used as counter and reference electrode. Material storage and sample preparations was performed in a dry room (dew point -65 °C). PEO was dried under vacuum (10<sup>-7</sup> mbar) at 45 °C and LiTFSI at 110 °C for 2 days before use. All other chemicals were used as received.

## 2.2. Linear Poly(ethylene oxide)-Based Solid Polymer Electrolyte Membrane Preparation

Linear PEO-based SPE polymer membranes were prepared by mixing of PEO (1 g) and LiTFSI (0.652 g) in in acetonitrile (6 g) using an EO:Li ratio of 10:1. The solvent was evaporated and the sample dried at 60 °C under reduced pressure ( $10^{-3}$  mbar). The resulting gum-like material was sandwiched between Mylar foil sheets and pressed at 100 °C with an applied pressure of 15 bar for 10 min. The thickness of the resulting membrane in the range of  $100 \pm 5 \, \mu m$  was controlled by the usage of a spacer.

## 2.3. Semi Interpenetrating Network Poly(ethylene oxide)-Based Solid Polymer Electrolyte Membrane Preparation

According to Scheme 1, the s-IPN PEO-based SPE was prepared by dissolving PEO (1 g), LiTFSI (0.878 g), PEGdMA ( $M_{\rm W}$  750 Da, 0.450 g, 45 wt%) and AIBN (0.046 g, 2 wt%) in acetonitrile (6 g) using an EO:Li ratio of 10:1. After homogenization, the solution was casted on mylar foil and the solvent was evaporated. The membrane was polymerized under N<sub>2</sub> flux at 80 °C for 1 h and dried over night at 80 °C under reduced pressure ( $10^{-3}$  mbar). [21] The concentration of PEGdMA was referred to the PEO content. The Li salt amount was adjusted to the MW of the used PEGdMA.

The successful formation of an s-IPN-type polymer electrolyte was characterized and proven by established gelation experiments.  $^{[22]}$  The principle is based on identification of the insoluble fraction (=network) of the membranes after extraction of the soluble fraction (linear PEO). Therefore, a sample of the polymer membrane was fixed in a stainless steel mesh and extracted using acetonitrile under stirring for 24 h. The solvent was discarded, the insoluble residue was dried under vacuum ( $10^{-7}$  mbar). Here, the residual weight could be attributed to 45 wt% PEGdMA content, thus to a successfully formed network.

#### 2.4. Electrode Preparation and Cell Assembly

NMC622 electrodes consisting of 91 wt% NMC622, 4 wt% carbon black, and 5 wt% PVdF were prepared by dissolving

PVdF in NMP followed by the addition of carbon black and NMC622. The mixture was homogenized using a dissolver. The slurry was casted on aluminum foil using a doctor blade with a wet coating thickness of 50 μm. The electrode sheets were dried for 3 h at 80 °C under vacuum, punched into circular electrode and dried again over night at 120 °C before use. The average active mass loading of NMC622 electrodes was 4.1 mg cm<sup>-2</sup>. For the LNMO electrodes, 84 wt% LNMO, 8 wt% carbon black, and 8 wt% PVdF were used. For the LMO electrodes 80 wt% LMO, 10 wt% carbon black, and 10 wt% PVdF were used. The LNMO and LMO electrodes were prepared using the procedure described above. The average active mass loading was 6.3 and 3.2 mg cm<sup>-2</sup>, respectively. All cells for galvanostatic cycling investigations were prepared in two electrode setup (coin cell) using ta NMC622 based positive electrode, [23] the PEO-based or the s-IPN PEO-based SPE as polymer membranes and lithium metal as negative electrode. Cells used for the determination of oxidative stability were prepared in three-electrode setup using the above mentioned positive electrodes as working electrode, and lithium metal as counter and reference electrode.

#### 2.5. Electrochemical Measurements

All constant current cycling experiments were conducted on a Maccor Series 4000 battery cell test system at 60 or 40 °C in a climate chamber (Binder KB400). The used C-rates and corresponding specific currents are mentioned within the text and/or in the figure captions.

#### 2.6. Differential Scanning Calorimetry

DSC measurements were performed using a TA Instruments Discovery DSC 2500 (TA Instruments, USA) in the temperature range of -100 to +120 °C with a scan rate of 10 °C min $^{-1}$ . The samples of  $\approx$ 2 mg were sealed in hermetic aluminum pans (TA Instruments, USA). Helium was used as sample gas (25 mL min $^{-1}$ ). Three cycles of heating and cooling within the given temperature range were performed.

#### 2.7. Mechanical Measurements

The compression behavior of the prepared SPE membranes was investigated using an Instron 5965 dual column universal testing machine (Instron, USA) with 50 mm compression plates. The samples were prepared by punching 18 mm discs of the SPE membranes with a thickness of  $\approx\!2$  mm. The measurements were performed with a speed of 20  $\mu m$  min $^{-1}$  at 20 °C.

#### 2.8. Atomic Force Microscopy

All atomic force microscopy (AFM) measurements were performed using a Cypher AFM (Asylum Research by Oxford Instruments, UK) with PPP-NCSTPt probes

www.afm-journal.de



(Nanosensors, Switzerland). The probes/membranes showed a nominal force constant in the range of 7.4 N m<sup>-1</sup> and were coated with a Pt/Ir alloy to ensure conductivity for Kelvin Probe Force Microscopy (KPFM) measurements. To ensure comparability, the same probe was used for all local measurements for both samples. All measurements were performed in air. The samples were stored in a desiccator between measurements to prevent surface deterioration due to humidity of oxidation. For image analysis, the programs Gwyddion 2.54 (GNU General Public License) and Pico Image Basix 7.4 (Digital Surf, France) were used. All images were obtained in intermittent contact mode and the topography as well as the phase shift of the mechanical vibration of the cantilever (mechanical characteristics of the sample surface) and the surface potential measured by KPFM were analyzed.

#### 2.9. Ionic Conductivity Measurements

Electrochemical impedance spectroscopy (EIS) was conducted utilizing an Autolab PGSTAT302N with FRA32M high frequency analyzer and MUX.SCNR16 16-fold multiplexer. The prepared SPE samples were sandwiched between stainless steel (SS) blocking electrodes and a PTFE spacer disc was used to keep the sample dimensions of 100  $\mu m$  height and 12 mm diameter constant in the coin cell (CR2032) housing. The sample cells were pre-heated at 70 °C for 2 h prior to the measurement to improve the surface wetting of the SS electrodes with the considered polymer samples. The EIS measurements were performed in the frequency range of 1 MHz to 1 Hz with an applied voltage amplitude of 10 mV in the temperature range of 0–80 °C in 5 °C steps. The temperature was controlled using a Binder MK53 climate chamber.

#### 3. Results and Discussion

#### 3.1. Increasing Li Salt Concentration

The variation of Li salt concentration in linear PEO-based SPEs is a compromise between high ionic conductivity and mechanical stability. This is related to the amount of poorly conducting but mechanically rigid crystalline domains of the SPE, which are diminishing with increasing the Li salt, owing to its plasticizing effect. [24] An excess in Li salt should be avoided as a certain amount of crystalline domains is essential for linear PEO-based SPEs to obtain a sufficient membrane robustness. This situation changes with a s-IPN PEO-based SPE, where the robustness does not solely depend on the amount of crystalline domains.

As depicted in **Figure 2**a, the ionic conductivity increases for the s-IPN PEO-based SPE with increasing salt concentration reaching a maximum for an EO:Li ratio of 10:1 at 40 °C. At 60 °C, the conductivity further grows with an increase of the Li salt concentration, whereas the conductivity at 40 °C remains constant for EO:Li ratios higher than 10:1, pointing toward a salt solubility limit, thus is considered as maximum salt concentration for this SPE. For comparison, as expected, the ionic conductivities for linear PEO-based SPE are higher for EO:Li ratio of 10:1, which are  $10^{-4.04}$  and  $10^{-3.52}$  S sm<sup>-1</sup> for 40 and 60 °C, respectively.

The highest raise in ionic conductivity can be found for salt concentrations corresponding to EO:Li ratios between 12:1 and 10:1. Considering data obtained from differential scanning calorimetry (DSC), this boost in conductivity can be related with a significant phase change of the SPE. As shown in Figure 2b, the melting peak of the crystalline domains at 40–50 °C shrinks with increasing salt concentration and even completely diminishes for an EO:Li ratio of 10:1. The absence of crystalline domains hints to a highly amorphous phase, which is beneficial for both, ionic conductivity and homogeneous Li plating.

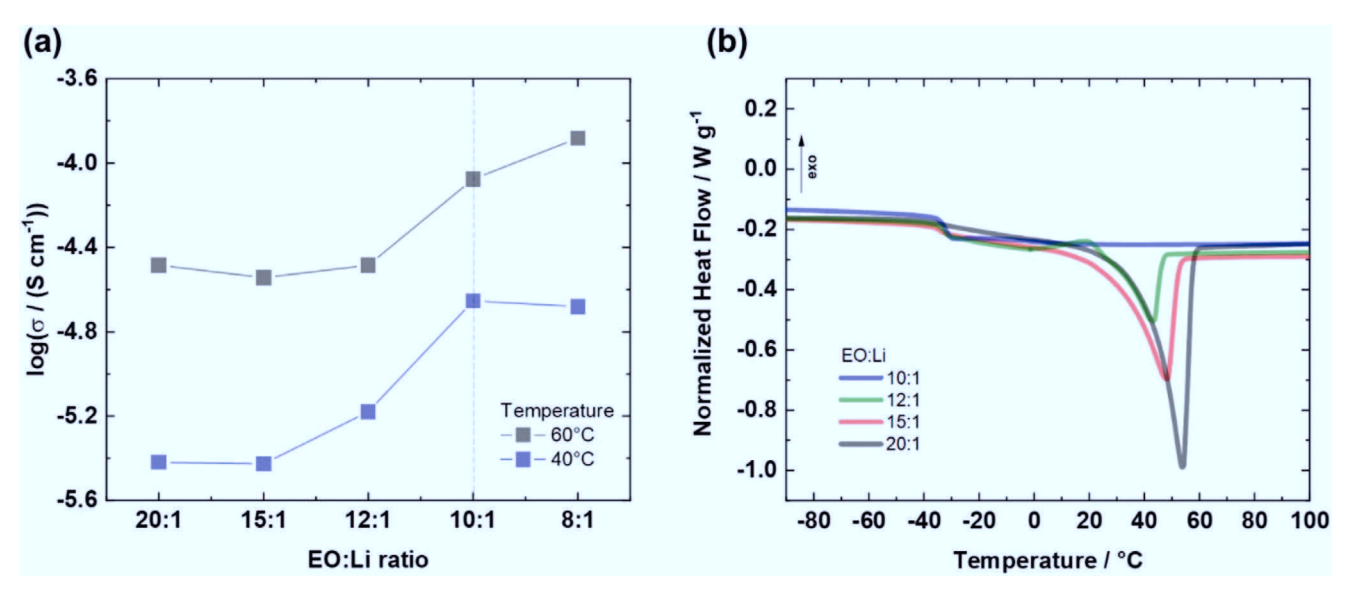


Figure 2. a) Ionic conductivities of the s-IPN PEO-based SPE as a function of Li salt concentration (EO:Li ratio) at 40 and 60 °C. The raise from 12:1 to 10:1 EO:Li is accompanied with highest increase in ionic conductivity. At 40 °C no gain in ionic conductivity is obtained for an EO:Li ratio higher than 10:1, thus can be regarded as solubility limit. b) Endothermic normalized heat flow measured by DSC of the s-IPN PEO-based SPE for varying salt concentrations as a function of temperature. The heat flow between 20 and 60 °C can be attributed to melting of crystalline domains. The increase in Li salt concentration leads to a decrease of crystalline domains, and even to their disappearance for an EO:Li ratio pf 10:1.

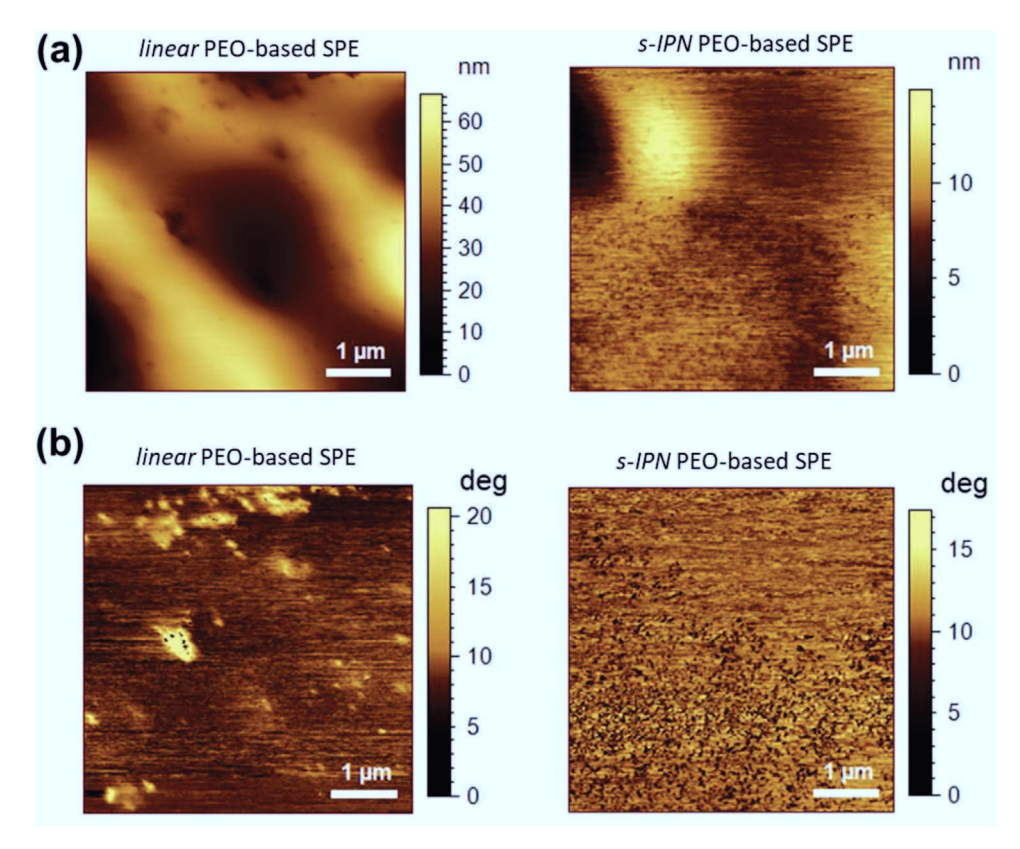


Figure 3. Exemplary surface images of the SPEs obtained by AFM. a) Topography demonstrates a significantly smoother surface for s-IPN PEO-based SPE with height deviations of ≈65 nm. b) Phase shift measurements: Only small deviation of the phase signal for the s-IPN PEO-based SPE imply a predominantly single phase contrary to the linear PEO-based SPE with more and uneven signal distribution. Overall, a more homogeneous and monophasic surface can be concluded for the s-IPN PEO-based SPE, which is in line with DSC data in Figure 2b.

The obtained highly amorphous phase can be related with increased homogeneity. Given its high sensitivity and at the same time the ability to distinguish phases, the visualization via AFM is doubly suitable to prove homogeneity and mono-phasic character of the network. The topographies of the SPEs with EO:Li 10:1 are shown in Figure 3a. While height differences of up to 65 nm for the linear PEO-based SPE are observed, the s-IPN PEO-based SPE reveals only height variations of up to 15 nm, suggesting a significantly smoother surface. More important, in line with the DSC results, the phase signal in Figure 3b shows an uneven distribution of phase shifts as seen by the dark color at ≈0 deg and yellow color at ≈20 deg, which pints to an unevenly distributed bi-phasic surface of the linear PEO-based SPE. For the s-IPN PEO-based SPE, an even distribution of an overwhelmingly one-phase shift can be observed at ≈12 deg, pointing to a monophasic and even surface. It can be concluded that the absence of crystalline domains in the SPE with optimized Li salt concentration (10:1 EO:Li) significantly improves ionic conductivity as well as surface homogeneity, rendering homogeneous Li plating likely. Given the Li dendrite penetration as a significant failure source in NMC622 | SPE | Li cells, particularly the improved homogeneity may act beneficial with respect to suppression of Li dendrite formation and growth. In total it may additionally contribute to a failure-free performance complementary to the essential mechanical and electrochemical aspects, which is part of next topic.

### 3.2. Mechanical and Electrochemical Stability of the Optimized Solid Polymer Electrolyte

Though the increased salt concentration has obvious benefits for ionic conductivity, mechanical and electrochemical stability must be ensured. A simple storage experiment at 60 °C can be informative for mechanical stability assessment, as shown in **Figure 4**a. Contrary to the linear PEO-based SPE, which melts and disintegrates, the s-IPN PEO-based SPE remains in its original shape. Hence, despite the absence of crystalline domains, the network prevents thermal deformation and point to sufficient mechanical stability.

To obtain deeper insights into mechanical aspects, compression tests are carried out for t both SPEs, which are depicted in Figure 4b. The onset of non-linear behavior of the compressive stress/strain behavior is regarded as irreversible sample deformation, thus can be regarded as mechanical stability limit.<sup>[25]</sup> The limit is significantly higher for the s-IPN PEO-based SPE (0.28 MPa) than for the linear PEO-based SPE (0.02 MPa), demonstrating its superior mechanical stability. It should be noted that the issue of Li dendrite penetration cannot solely depend on mechanical aspects and the significance of other properties, for example, homogeneity should not be disregarded.

A further crucial requirement for battery cell operation of the SPE is its electrochemical stability. For an assessment of application relevance and validity, a galvanostatic



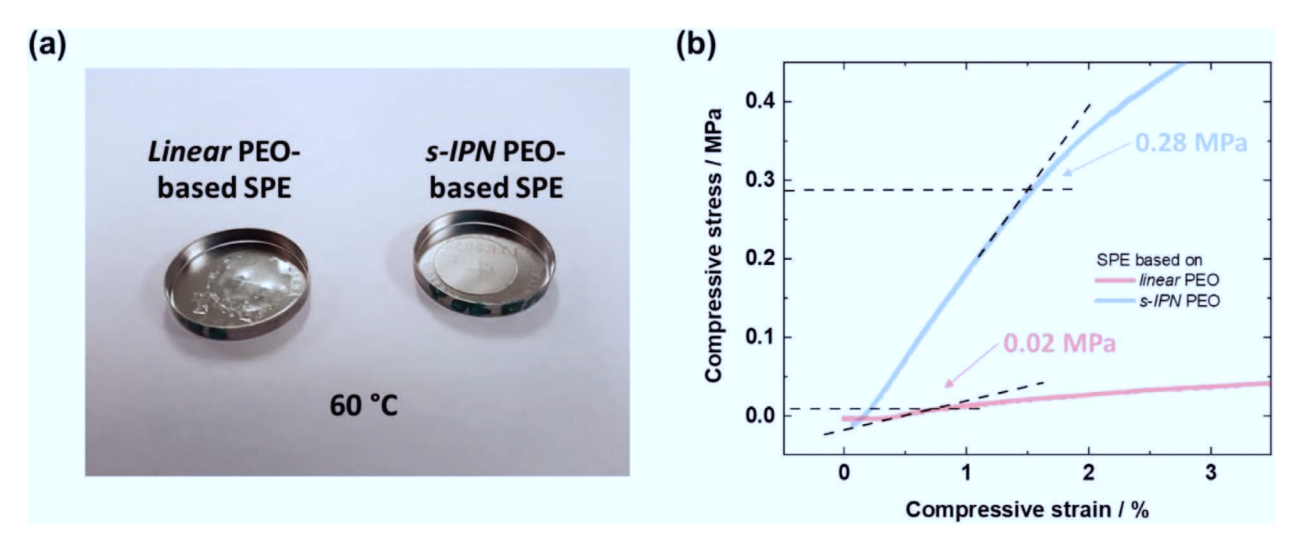


Figure 4. Stability tests for linear PEO- and s-IPN PEO-based SPEs for with an EO:Li ratio of 10:1 at 60 °C. a) Photograph of both SPEs in coin cell cups after storage for 7 days. Contrary to linear PEO-based SPE, the s-IPN PEO-based SPE remains solid in original shape. b) Mechanical data for both SPEs obtained from compression tests. The stability limit for s-IPN PEO-based SPE is significantly higher (0.28 MPa) compared to linear PEO-based SPE (0.02 MPa), demonstrating the s-IPN PEO-based SPE as a free-standing and stable membrane even at 60 °C.

overcharge experiment is carried out in composite electrodes using LiMn<sub>2</sub>O<sub>4</sub> (LMO) and LiNi<sub>0.5</sub>Mn<sub>1.5</sub>O<sub>4</sub> (LNMO), which represents overcharge stable active materials with and without Ni (to exclude possible catalytic activity). [26–28] As seen in **Figure 5**a, after the typical LMO delithiation process at potentials between 3.9 and 4.3 V versus Li  $\mid$  Li<sup>+</sup>,[29,30] the potential plateaus at ~4.6 V versus Li  $\mid$  Li<sup>+</sup> indicate a similar oxidation onset for both SPEs. A similar potential plateau is also observed on the LNMO electrode, as depicted in Figure 5b. The parasitic decomposition reaction of the SPE prevents further LNMO delithiation, which is known to occur in typical organic solvent based liquid electrolytes at 4.7 and 4.9 V versus Li Li<sup>+</sup>. Both SPEs consequently reveal similar

electrochemical stabilities, which are sufficiently high for NMC622 | SPE | Li cells with upper charge cut-off voltages of typically below 4.3 V. Again, the typical random appearance of the voltage noise failure is seen for the linear PEO-based SPE.

## 3.3. Optimized Solid Polymer Electrolyte: Electrochemical Performance in LiNi<sub>0.6</sub>Mn<sub>0.2</sub>Co<sub>0.2</sub>O<sub>2</sub> | Solid Polymer Electrolyte | Li Cell

The results so far strongly point at the fact, that the crucial point for a "voltage noise"-free performance in an NMC622 | SPE | Li cell is predominantly related to the physical

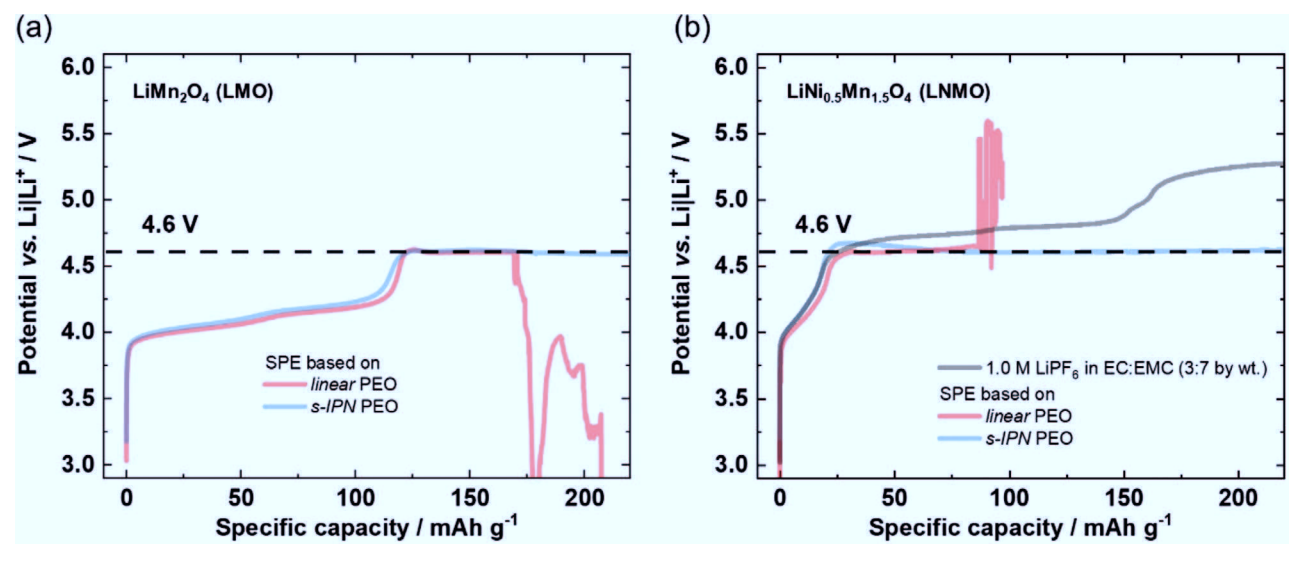


Figure 5. Anodic stabilities obtained by galvanostatic overcharge experiments for both SPEs with an EO:Li ratio of 10:1 at 60 °C with a specific current of 15 mA g<sup>-1</sup> using a) Ni-free and b) Ni-containing composite spinel electrodes. a) After delithiation of LMO between 3.9 and 4.3 V versus Li | Li<sup>+</sup>, the charge process ends with a plateau at 4.6 V versus Li | Li<sup>+</sup> for both SPEs. b) Similar plateaus are observed with LNMO electrodes. The formation of this plateau prevents the electrode from reaching the characteristic charge process of LNMO between 4.7 and 4.9 V versus Li | Li<sup>+</sup>. Independent of the electrode material composition, both SPEs reveal similar oxidation onsets of 4.6 V versus Li | Li<sup>+</sup>.

www.advancedsciencenews.com www.afm-journal.de

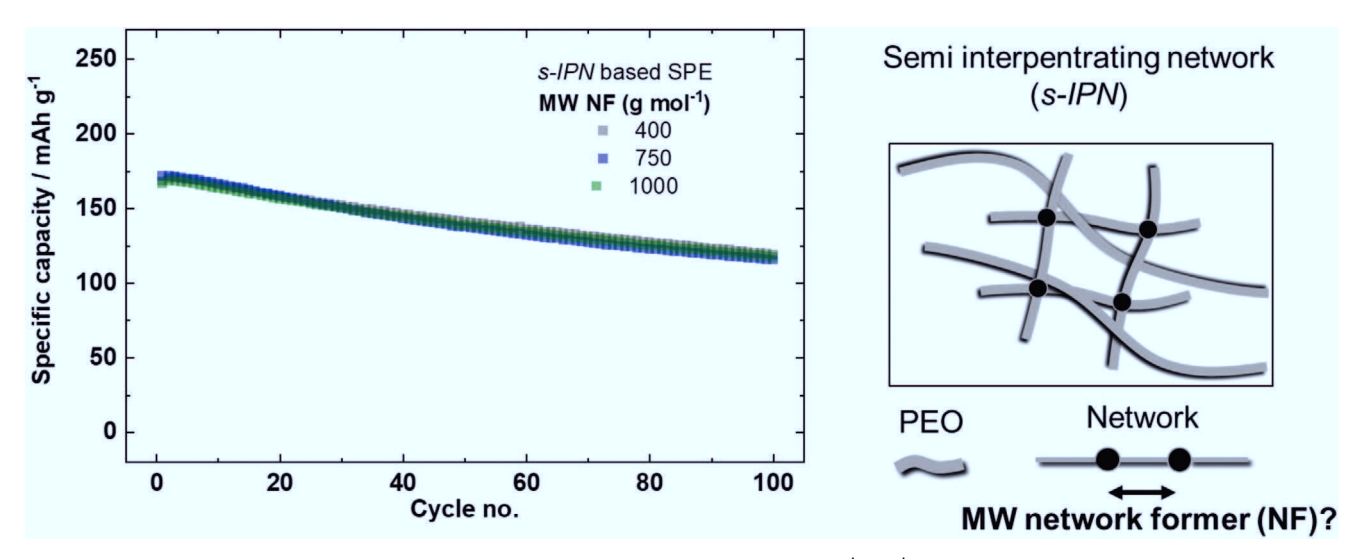


Figure 6. Charge/discharge cycling performance of the s-IPN PEO-based SPE in an NMC622 | SPE | Li cell (4.3–3.0 V, 30 mA g<sup>-1</sup>) for varied molecular weights (MW) of the network former (NF). A variation of the amount of NF agents (lower for higher MW) does not influence the performance. Independent of the MW, the charge/discharge cycling performance proceeds without "voltage noise" failure, in contrast to the linear PEO-based SPE.

prevention of Li dendrite reasoned micro short circuits. To exclude a possible chemical impact originating from the network former based on methacrylate groups, the molecular weight, thus the length of the PEO backbone, of the network former is varied.

With increasing  $M_{W_0}$ , the amount of methacrylate decreases and vice versa. The charge/discharge cycling performance in an NMC622 | SPE | Li cell for the s-IPN PEO-based SPE with a  $M_{\rm W}$ of the NF = 400, 750, and 1000 g  $\text{mol}^{-1}$  is depicted in Figure 6. The performance is not affected by the  $M_W$ , which neglects the chemical impact of the NF and the sensitivity of the s-IPN with regard to overall performance.

The impact of the salt optimized s-IPN SPE ( $\sigma = 10^{-4.65} \text{ S cm}^{-1}$ ) with an EO:Li ratio of 10:1 on the overall charge/discharge cycling performance is investigated in comparison to a non-optimized SPE ( $\sigma = 10^{-5.43}$  S cm<sup>-1</sup>) with an EO:Li ratio of 15:1, at 40 °C. The optimized SPE demonstrates significantly higher specific capacities (Figure 7). Continuous charge/discharge cycling without any aberrations in specific charge capacities distinctly demonstrate absence of any "voltage noise" and point to an effective suppression of Li dendrite penetration for both s-IPN PEO-based SPEs.[16] The optimized SPE generates significantly higher capacities. Though, higher ionic conductivities are known in literature, [31,32] the here shown specific capacities are interestingly still high implying that ionic conductivities are obviously not the only crucial parameter for the overall performance and other parameter (e.g., wettability) should not be disregarded when comparing different electrolyte systems. In other words, better ionic conductivities do not necessarily guarantee better performance.<sup>[33]</sup> Nevertheless, within the same SPE, the difference in ionic conductivity can play a crucial role. Here, they significantly affect the specific capacities and coulombic efficiencies (specific capacity losses) in the initial cycle, which is characteristic for NMC-based electrodes due to kinetic origin.[13,14,34]

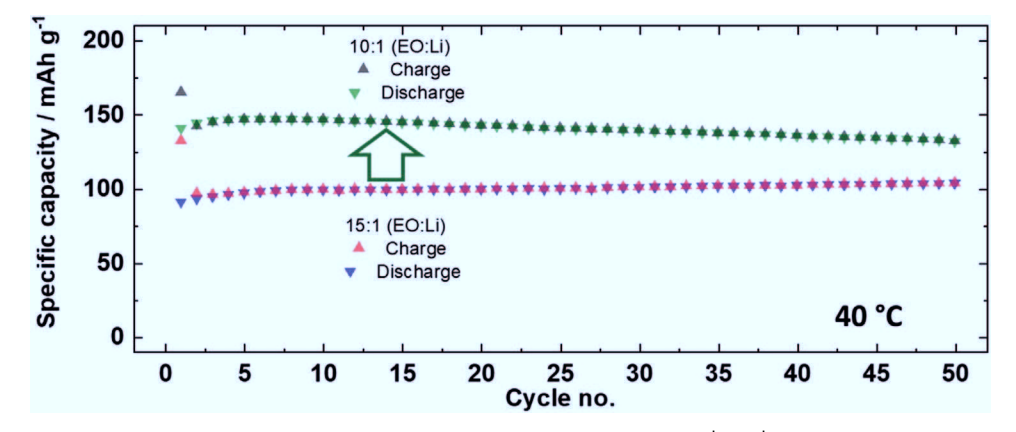


Figure 7. Charge/discharge cycling performance of two different s-IPN based SPEs in a NMC622 SPE Li cell (4.3-3.0 V, 15 mA g<sup>-1</sup>) for the improved Li salt concentration with EO:Li ratio of 10:1 in comparison to a not-optimized SPE with an EO:Li ratio at 15:1. The optimized SPE reveals a significant performance increase, even at 40 °C.

www.afm-journal.de



SPEs based on conventional linear PEO show a "voltage noise" failure in LMBs when using high energy/high voltage electrodes like NMC622, which is caused by Li dendrite induced short circuits. The integration of the PEO-based SPE in a s-IPN prevents this failure and enables continuous "voltage noise"-free charge/discharge cycling in NMC622 | SPE | Li cells.

The mechanically rigid network of the s-IPN empowers novel SPE design opportunities making the presence of rigid crystalline domains not essential anymore. By increasing the amount of the plasticizing Li salt in the SPE toward an EO:Li ratio of 10:1 the crystalline domains can be suppressed as confirmed via DSC. The change toward the highly amorphous phase results in a boost of ionic conductivity and into a more homogeneous and smoother surface, as demonstrated by EIS and atomic force microscopy, respectively.

Despite the suppressed crystalline domains, the membrane of the optimized s-IPN PEO-based SPE remains solid in original shape even after storage at 60 °C for 7 days, and still provides superior mechanical properties as measured by means of compression tests. Also, no detrimental effect on anodic stability is observed, still demonstrating high stabilities up to 4.6 V versus Li | Li<sup>+</sup> at Ni-free and Ni-containing composite spinel electrodes in a galvanostatic manner. The optimized SPE shows comparatively good cycling stability at high discharge capacities in NMC622 | SPE | Li cells, even at 40 °C.

Finally, the here shown failure of high voltage LMBs with PEO-based SPEs counterintuitively depends less on the electrochemical aspects, but obviously on aspects associated with Li dendrite penetration. In this regard, it is shown that not only mechanical properties but also homogeneity properties should not be disregarded for an SPE design.

#### Acknowledgements

Financial support from the German Federal Ministry for Education and Research within the project FestBatt (grant number: 13XP0175A) is gratefully acknowledged. Open access funding enabled and organized by Projekt DEAL.

#### **Conflict of Interest**

The authors declare no conflict of interest.

#### **Keywords**

high voltage NMC, Li metal batteries, poly(ethylene oxide), semi interpenetration network, solid polymer electrolytes

Received: July 26, 2020 Published online:

- [3] G. Homann, P. Meister, L. Stolz, J. P. Brinkmann, J. Kulisch, T. Adermann, M. Winter, J. Kasnatscheew, ACS Appl. Energy Mater. 2020, 3, 3162
- [4] R. Schmuch, R. Wagner, G. Hörpel, T. Placke, M. Winter, Nat. Energy 2018, 3, 267.
- [5] J. Schnell, T. Gunther, T. Knoche, C. Vieider, L. Kohler, A. Just, M. Keller, S. Passerini, G. Reinhart, J. Power Sources 2018, 382, 160.
- [6] F. B. Dias, L. Plomp, J. B. J. Veldhuis, J. Power Sources 2000, 88, 169.
- [7] J. Janek, W. G. Zeier, Nat. Energy 2016, 1, 16141.
- [8] K. Kerman, A. Luntz, V. Viswanathan, Y. M. Chiang, Z. B. Chen, J. Electrochem. Soc. 2017, 164, A1731.
- [9] T. Placke, R. Kloepsch, S. Dühnen, M. Winter, J. Solid State Electrochem. 2017, 21, 1939.
- [10] J. R. Nair, L. Imholt, G. Brunklaus, M. Winter, Electrochem. Soc. Interface 2019, 28, 55.
- [11] Z. Wan, D. Lei, W. Yang, C. Liu, K. Shi, X. Hao, L. Shen, W. Lv, B. Li, Q.-H. Yang, F. Kang, Y.-B. He, Adv. Funct. Mater. 2019, 29, 1805301.
- [12] J. Kasnatscheew, S. Röser, M. Börner, M. Winter, ACS Appl. Energy Mater. 2019, 2, 7733.
- [13] J. Kasnatscheew, M. Evertz, B. Streipert, R. Wagner, S. Nowak, I. C. Laskovic, M. Winter, J. Power Sources 2017, 359, 458.
- [14] J. Kasnatscheew, M. Evertz, R. Kloepsch, B. Streipert, R. Wagner, I. C. Laskovic, M. Winter, *Energy Technol.* 2017, 5, 1670.
- [15] J. Mindemark, M. J. Lacey, T. Bowden, D. Brandell, *Prog. Polym. Sci.* 2018, 81, 114.
- [16] G. Homann, L. Stolz, J. Nair, I. C. Laskovic, M. Winter, J. Kasnatscheew, Sci. Rep. 2020, 10, 4390.
- [17] G. Bieker, M. Winter, P. Bieker, Phys. Chem. Chem. Phys. 2015, 17, 8670.
- [18] J. Heine, P. Hilbig, X. Qi, P. Niehoff, M. Winter, P. Bieker, J. Electrochem. Soc. 2015, 162, A1094.
- [19] D. Zhou, R. Liu, Y.-B. He, F. Li, M. Liu, B. Li, Q.-H. Yang, Q. Cai, F. Kang, Adv. Energy Mater. 2016, 6, 1502214.
- [20] A. Gupta, E. Kazyak, N. Craig, J. Christensen, N. P. Dasgupta, J. Sakamoto, J. Electrochem. Soc. 2018, 165, A2801.
- [21] G. Homann, L. Stolz, M. Winter, J. Kasnatscheew, iScience 2020, 23, 101225.
- [22] J. R. Nair, M. Destro, F. Bella, G. B. Appetecchi, C. Gerbaldi, J. Power Sources 2016, 306, 258.
- [23] R. Nölle, K. Beltrop, F. Holtstiege, J. Kasnatscheew, T. Placke, M. Winter, Mater. Today 2020, 32, 131.
- [24] W. A. Henderson, Macromolecules 2007, 40, 4963.
- [25] M. L. Lehmann, G. Yang, D. Gilmer, K. S. Han, E. C. Self, R. E. Ruther, S. Ge, B. Li, V. Murugesan, A. P. Sokolov, F. M. Delnick, J. Nanda, T. Saito, Energy Storage Mater. 2019, 21, 85.
- [26] J. Kasnatscheew, B. Streipert, S. Röser, R. Wagner, I. C. Laskovic, M. Winter, Phys. Chem. Chem. Phys. 2017, 19, 16078.
- [27] K. Xu, S. P. Ding, T. R. Jow, J. Electrochem. Soc. 1999, 146, 4172.
- [28] M. S. Whittingham, Chem. Rev. 2004, 104, 4271.
- [29] P. Janssen, J. Kasnatscheew, B. Streipert, C. Wendt, P. Murmann, M. Ponomarenko, O. Stubbmann-Kazakova, G.-V. Röschenthaler, M. Winter, I. Cekic-Laskovic, J. Electrochem. Soc. 2018, 165, A3525.
- [30] J. Kasnatscheew, M. Evertz, B. Streipert, R. Wagner, R. Klopsch, B. Vortmann, H. Hahn, S. Nowak, M. Amereller, A. C. Gentschev, P. Lamp, M. Winter, *Phys. Chem. Chem. Phys.* **2016**, *18*, 3956.
- [31] W. Tang, S. Tang, X. Guan, X. Zhang, Q. Xiang, J. Luo, Adv. Funct. Mater. 2019, 29, 1900648.
- [32] W. Tang, S. Tang, C. Zhang, Q. Ma, Q. Xiang, Y.-W. Yang, J. Luo, Adv. Energy Mater. 2018, 8, 1800866.
- [33] J. Kasnatscheew, U. Rodehorst, B. Streipert, S. Wiemers-Meyer, R. Jakelski, R. Wagner, I. C. Laskovic, M. Winter, J. Electrochem. Soc. 2016, 163, A2943.
- [34] J. Kasnatscheew, M. Evertz, B. Streipert, R. Wagner, S. Nowak, I. C. Laskovic, M. Winter, J. Phys. Chem. C 2017, 121, 1521.

H. S. Shin, W. G. Ryu, M. S. Park, K. N. Jung, H. Kim, J. W. Lee, *ChemSusChem* 2018, 11, 3184.

<sup>[2]</sup> K. N. Jung, H. S. Shin, M. S. Park, J. W. Lee, ChemElectroChem 2019, 6, 3842.